2016 American Control Conference (ACC)
Boston Marriott Copley Place
July 6-8, 2016. Boston, MA, USA

Nonlinear Passivity-Based Adaptive Control of Spacecraft Formation Flying

Steve Ulrich[1]

Abstract— **In this paper, a nonlinear output feedback adaptive control system for spacecraft formation flying is developed. Specifically, the proposed approach addresses the problem of controlling a chaser spacecraft such that it tracks a desired relative trajectory with respect to the target spacecraft, regardless of unknown parameters and disturbance forces. Making use of passivity results, the closed-loop stability of the adaptive system is guaranteed via Lyapunov direct method and LaSalle's invariance principle arguments. Simulation results for a projected circular formation example are provided to illustrate the increased performance and robustness of the proposed adaptive controller compared to a conventional non-adaptive proportional-derivative control law.**

I. INTRODUCTION

Over the last two decades, there has been a growing research interest in the area of dynamics and control of spacecraft formation flying. Several formation flying control laws were derived based on nonlinear control techniques, such as the state-dependent Ricatti equation method [1] and the feedback linearization technique [2]. In addition, adaptive control laws were proposed to specifically address the problem of relative motion tracking between two spacecraft under parametric uncertainties and unknown disturbances. de Queiroz et al. [3] and Wong et al. [4] proposed adaptive state-feedback lineariztion controllers in which on-line estimation of unknown parameters and disturbances are employed. Nonlinear adaptive variable-structure state-feedback control techniques were investigated by Shahid and Kumar [5] and Godard and Kumar [6]. Besides required full state feedback, all aforementioned adaptive control techniques represent *indirect adaptive control* methodologies which consist in estimating the uncertain plant parameters and unknown disturbances. An adverse consequence of such on-line procedures is the increased computational burden associated with real-time estimation of unknown parameters. Alternatively, *direct adaptive control* methodologies that do not require estimates of unknown plant parameters can be used to address this problem. To this end, an output feedback approach based on the variable-structure model reference adaptive control theory was developed by Lee and Singh [7]. However, their technique nevertheless requires two-first order filters, one averaging filter, and two relays along with their related modulation functions, which complexifies the overall control system.

In view of the above, the main contribution of this paper is the design of a simple nonlinear direct adaptive output feedback approach that, unlike most existing adaptive techniques for spacecraft formation flying, do not require on-line estimation identification of unknown parameters and disturbances. The development is based on a new class of direct adaptive output feedback controllers for nonlinear square systems, termed decentralized simple adaptive control (DSAC) theory, which has been developed in the context of flexible-joint robot manipulator control [8], [9]. The DSAC methodology differs from the conventional SAC method in the control gain adaptation laws, which are *decentralized* in the sense that they consider only the diagonal elements. By omitting the cross couplings, each axis is controlled separately and independently, which make the new decentralized approaches better suited for real-time applications with low computational power, such as small spacecraft platforms.

II. ALMOST STRICTLY PASSIVE RELATIVE DYNAMICS

This section presents the exact nonlinear equations of motion that model the spacecraft relative dynamics, upon which the passivity-based adaptive controller will be designed. Following common practice, the relative equations of motion are expressed in the local-vertical-local-horizontal (LVLH) reference frame, denoted by $\mathcal{F}_L$ and defined with its origin located at the target spacecraft, with its $\vec{L}_x$ unit vector in the direction of the target position vector $\vec{r}_t$, its $\vec{L}_z$ unit vector perpenticular to the orbital plane, and its $\vec{L}_y$ unit vector completing the triad.

Let express the relative position vector $\vec{\rho}$ in terms of its components in $\mathcal{F}_L$ as

$$\vec{\rho} = \vec{r}_c - \vec{r}_t = \vec{\mathcal{F}}_L^T \begin{bmatrix} x \\ y \\ z \end{bmatrix} \tag{1}$$

where $\vec{r}_c$ represents the inertial chaser position vector, $r_t = |\vec{r}_t|$, and where the $\{x, y\}$ components of $\vec{\rho}$ respectively denote the radial and along-track components and describe the relative motion in the target orbital plane, and where the z component is referred to as the cross-track component that describes the relative motion out of the target orbital plane. Treating both spacecraft as point masses and equating the two-body equation of motion for the chaser spacecraft in LVLH to the kinematic acceleration of the chaser spacecraft yields, after some algebraic manipulations, the exact, nonlinear equations of motion that describe the components of the relative acceleration vector in $\mathcal{F}_L$ [6]

[1]Steve Ulrich is with the Department of Mechanical and Aerospace Engineering, Carleton University, Ottawa, Ontario, K1S 5B6 (email: steve.ulrich@carleton.ca)

$$\ddot{x} - \dot{\theta}^2 x - 2\dot{\theta}\dot{y} - \ddot{\theta} y + \mu \left(\frac{r_t + x}{r_c^3} - \frac{1}{r_t^2} \right) = a_x \quad (2)$$

$$\ddot{y} - \dot{\theta}^2 y + 2\dot{\theta}\dot{x} + \ddot{\theta} x + \frac{\mu}{r_c^3} y = a_y \quad (3)$$

$$\ddot{z} + \frac{\mu}{r_c^3} z = a_z \quad (4)$$

with

$$\ddot{r}_t = \dot{\theta}^2 r_t - \frac{\mu}{r_t^2} \quad (5)$$

$$\ddot{\theta} = -2\frac{\dot{r}_t}{r_t}\dot{\theta} \quad (6)$$

and where θ is the true anomaly of the target spacecraft, μ is the constant gravitational parameter of the Earth, $r_c = |\vec{r}_c| = \sqrt{(r_t + x)^2 + y^2 + z^2}$, and $a_j = f_j/m_c \ \forall j = \{x, y, z\}$, with m_c denoting the mass of the chaser spacecraft, and f_j denoting the control input applied by the chaser spacecraft.

For convenience, let formulate the dynamics equations of motion as a square nonlinear state-space model

$$\dot{\boldsymbol{x}} = \boldsymbol{A}(\boldsymbol{x})\boldsymbol{x} + \boldsymbol{B}\boldsymbol{u} + \boldsymbol{G}(\boldsymbol{x}), \qquad \boldsymbol{y} = \boldsymbol{C}\boldsymbol{x} \quad (7)$$

with the states $\boldsymbol{x} \in \mathbb{R}^6$, inputs $\boldsymbol{u} \in \mathbb{R}^3$, and scaled-position-plus-velocity outputs $\boldsymbol{y} \in \mathbb{R}^3$ respectively defined as

$$\boldsymbol{x} = \left[\begin{array}{cccccc} x & y & z & \dot{x} & \dot{y} & \dot{z} \end{array} \right]^T \quad (8)$$

$$\boldsymbol{u} = \left[\begin{array}{ccc} f_x & f_y & f_z \end{array} \right]^T \quad (9)$$

$$\boldsymbol{y} = \left[\begin{array}{ccc} \alpha x + \dot{x} & \alpha y + \dot{y} & \alpha z + \dot{z} \end{array} \right]^T \quad (10)$$

where α is a known positive-definite scaling gain. The appropriately-dimensioned real matrices $\boldsymbol{A}(\boldsymbol{x})$, $\boldsymbol{B}$, $\boldsymbol{G}(\boldsymbol{x})$, and $\boldsymbol{C}$ are then

$$\boldsymbol{A}(\boldsymbol{x}) = \left[\begin{array}{cccccc} 0 & 0 & 0 & 1 & 0 & 0 \\ 0 & 0 & 0 & 0 & 1 & 0 \\ 0 & 0 & 0 & 0 & 0 & 1 \\ \dot{\theta}^2 - \frac{\mu}{r_c^3} & \ddot{\theta} & 0 & 0 & 2\dot{\theta} & 0 \\ -\ddot{\theta} & \dot{\theta}^2 - \frac{\mu}{r_c^3} & 0 & -2\dot{\theta} & 0 & 0 \\ 0 & 0 & -\frac{\mu}{r_c^3} & 0 & 0 & 0 \end{array} \right] \quad (11)$$

$$\boldsymbol{B} = \left[\begin{array}{cccccc} 0 & 0 & 0 & \frac{1}{m_c} & 0 & 0 \\ 0 & 0 & 0 & 0 & \frac{1}{m_c} & 0 \\ 0 & 0 & 0 & 0 & 0 & \frac{1}{m_c} \end{array} \right]^T \quad (12)$$

$$\boldsymbol{G}(\boldsymbol{x}) = \left[\begin{array}{cccccc} 0 & 0 & 0 & \mu\left(\frac{1}{r_t^2} - \frac{r_t}{r_c^3}\right) & 0 & 0 \end{array} \right]^T \quad (13)$$

$$\boldsymbol{C} = \left[\begin{array}{cc} \alpha \boldsymbol{I}_3 & \boldsymbol{I}_3 \end{array} \right] \quad (14)$$

Property 1. The nonlinear spacecraft formation flying dynamics model expressed as a square state-space system by Eq. (7) with matrices in Eqs. (11)-(14) is uniformly strictly minimum phase.

Proof. A nonlinear system is said uniformly strictly minimum phase if its zero dynamics is uniformly stable [10]. In other words, there exist two constant matrices $\boldsymbol{M} \in \mathbb{R}^{6\times 3}$ and $\boldsymbol{N} \in \mathbb{R}^{3\times 6}$ that satisfies

$$\boldsymbol{C}\boldsymbol{M} = \boldsymbol{0}_3 \quad (15)$$

$$\boldsymbol{N}\boldsymbol{B} = \boldsymbol{0}_3 \quad (16)$$

$$\boldsymbol{N}\boldsymbol{M} = \boldsymbol{I}_3 \quad (17)$$

so that the zero dynamics given by

$$\dot{\boldsymbol{z}} = \boldsymbol{A}_z(\boldsymbol{x})\boldsymbol{z} \in \mathbb{R}^3 \quad (18)$$

is uniformly asymptotically stable, where $\boldsymbol{A}_z(\boldsymbol{x}) \in \mathbb{R}^{3\times 3}$ is the zero dynamics system matrix

$$\boldsymbol{A}_z(\boldsymbol{x}) = \boldsymbol{N}\boldsymbol{A}(\boldsymbol{x})\boldsymbol{M} \quad (19)$$

Two matrices $\boldsymbol{M}$ and $\boldsymbol{N}$ that satifies Eqs. (15)-(17) are

$$\boldsymbol{M} = \left[\begin{array}{c} \boldsymbol{I}_3 \\ -\alpha \boldsymbol{I}_3 \end{array} \right], \quad \boldsymbol{N} = \left[\begin{array}{cc} \boldsymbol{I}_3 & \boldsymbol{0}_3 \end{array} \right] \quad (20)$$

As a result, the zero dynamics matrix $\boldsymbol{A}_z$ is

$$\boldsymbol{A}_z = \boldsymbol{N}\boldsymbol{A}(\boldsymbol{x})\boldsymbol{M} = -\alpha \boldsymbol{I}_3 \quad (21)$$

such that the zero dynamics is

$$\dot{\boldsymbol{z}} = -\alpha \boldsymbol{z} \quad (22)$$

which demonstrates that the zero dynamics is stable and that the relative motion dynamics is uniformly strictty minimum phase.

□

Definition 1. A nonlinear, uniformly strictly minimum phase system and with the product $\boldsymbol{C}\boldsymbol{B}$ being positive definite symmetric (PDS) is said to be almost strictly passive (ASP), and thus simultaneously satisfies the two ASP conditions

$$\dot{\boldsymbol{P}}(\boldsymbol{x}) + \boldsymbol{P}(\boldsymbol{x})\left(\boldsymbol{A}(\boldsymbol{x}) - \boldsymbol{B}\tilde{\boldsymbol{K}}_e\boldsymbol{C}\right) + \left(\boldsymbol{A}(\boldsymbol{x}) - \boldsymbol{B}\tilde{\boldsymbol{K}}_e\boldsymbol{C}\right)^T \boldsymbol{P}(\boldsymbol{x}) = -\boldsymbol{Q}(\boldsymbol{x}) \quad (23)$$

$$\boldsymbol{P}(\boldsymbol{x})\boldsymbol{B} = \boldsymbol{C}^T \quad (24)$$

where $\boldsymbol{P}(\boldsymbol{x})$ and $\boldsymbol{Q}(\boldsymbol{x})$ are two PDS matrices, and $\tilde{\boldsymbol{K}}_e$ is a constant output feedback gain matrix [10].

Property 2. The nonlinear spacecraft formation flying dynamics model expressed as a square state-space system by Eq. (7) with matrices in Eqs. (11)-(14) is ASP.

Proof. The product of the output and input matrices **CB** is positive definite symmetric (PDS)

$$\boldsymbol{CB} = \begin{bmatrix} \alpha\boldsymbol{I}_3 & \boldsymbol{I}_3 \end{bmatrix} \begin{bmatrix} 0 & 0 & 0 \\ 0 & 0 & 0 \\ 0 & 0 & 0 \\ \frac{1}{m_c} & 0 & 0 \\ 0 & \frac{1}{m_c} & 0 \\ 0 & 0 & \frac{1}{m_c} \end{bmatrix} = \frac{1}{m_c}\boldsymbol{I}_3 \tag{25}$$

Invoking Property 1 and Definition 1 completes the proof.

□

III. PROBLEM FORMULATION

The control problem addressed in this paper is an output feedback model following problem that consists in calculating the control input force $\boldsymbol{u} = \begin{bmatrix} f_x & f_y & f_z \end{bmatrix}^T$ such that the plant outputs $\boldsymbol{y}$ tracks, in the presence of external disturbances, initial deployment errors that would generate undesirable dispersion of the formation when left uncontrolled, and unknown chaser mass, the outputs $\boldsymbol{y}_m \in \mathbb{R}^3$ of an ideal model herein represented as linear-time-invariant system

$$\dot{\boldsymbol{x}}_m = \boldsymbol{A}_m\boldsymbol{x}_m + \boldsymbol{B}_m\boldsymbol{u}_m, \qquad \boldsymbol{y}_m = \boldsymbol{C}_m\boldsymbol{x}_m \tag{26}$$

with the states $\boldsymbol{x}_m \in \mathbb{R}^6$, inputs $\boldsymbol{u}_m \in \mathbb{R}^3$, and outputs $\boldsymbol{y}_m$ of the ideal model herein defined as

$$\boldsymbol{x}_m = \begin{bmatrix} x_m & y_m & z_m & \dot{x}_m & \dot{y}_m & \dot{z}_m \end{bmatrix}^T \tag{27}$$

$$\boldsymbol{u}_m = \begin{bmatrix} x_d & y_d & z_d \end{bmatrix}^T \tag{28}$$

$$\boldsymbol{y}_m = \begin{bmatrix} \alpha x_m + \dot{x}_m & \alpha y_m + \dot{y}_m & \alpha z_m + \dot{z}_m \end{bmatrix}^T \tag{29}$$

where $\left\{ x_d \quad y_d \quad z_d \right\}$ denote the components of the desired relative position vector in $\mathcal{F}_L$ and, in this paper, correspond to a projected circular orbit (PCO), which describes a circular trajectory with a constant separation in the along-track/cross-track plane, i.e., in the $\vec{L}_y - \vec{L}_z$ plane. In other words, with the PCO, the three-dimensional ellipse of relative motion projected on to the along-track/cross-track plane gives a circle mathematically described by $y_d^2 + z_d^2 = r_{pco}^2$.

$$\boldsymbol{u}_m = \begin{bmatrix} x_d \\ y_d \\ z_d \end{bmatrix} = \frac{r_{pco}}{2}\begin{bmatrix} \sin(nt) \\ 2\cos(nt) \\ 2\sin(nt) \end{bmatrix} \tag{30}$$

where r_{pco} denotes the size of the PCO, $n = \sqrt{\mu/a^3}$ is the mean orbital motion, and a is the semi-major axis of the target spaceraft orbit. The desired closed-loop relative motion response to these inputs is characterized through the ideal model matrices $\boldsymbol{A}_m$, $\boldsymbol{B}_m$ and $\boldsymbol{C}_m$

$$\boldsymbol{A}_m = \begin{bmatrix} 0 & 0 & 0 & 1 & 0 & 0 \\ 0 & 0 & 0 & 0 & 1 & 0 \\ 0 & 0 & 0 & 0 & 0 & 1 \\ -\omega_n^2 & 0 & 0 & -2\zeta\omega_n & 0 & 0 \\ 0 & -\omega_n^2 & 0 & 0 & -2\zeta\omega_n & 0 \\ 0 & 0 & -\omega_n^2 & 0 & 0 & -2\zeta\omega_n \end{bmatrix}$$

$$\boldsymbol{B}_m = \begin{bmatrix} 0 & 0 & 0 & \omega_n^2 & 0 & 0 \\ 0 & 0 & 0 & 0 & \omega_n^2 & 0 \\ 0 & 0 & 0 & 0 & 0 & \omega_n^2 \end{bmatrix}^T$$

$$\boldsymbol{C}_m = \begin{bmatrix} \alpha\boldsymbol{I}_3 & \boldsymbol{I}_3 \end{bmatrix}$$

where ζ and ω_n respectively denote the ideal damping ratio and undamped natural frequency ω_n. This ideal model thus only represents the desired, or ideal, input-output closed-loop behavior of the relative motion, and is not based on any explicit *a priori* knowledge about the dynamics parameters.

The model output following objective is quantified through the output tracking error, denoted by $\boldsymbol{e}_y \in \mathbb{R}^3$, is defined as

$$\boldsymbol{e}_y \triangleq \boldsymbol{y}_m - \boldsymbol{y} \tag{31}$$

Because the parameter m_c and external disturbances, denoted by F_{dj} $\forall j = \{x, y, z\}$, are assumed to be unknown, the control law presented in the next section employs direct adaptation laws that vary the controller gains in response to the tracking error $\boldsymbol{e}_y$, without requiring on-line estimates of m_c and/or F_{dj}.

IV. PASSIVITY-BASED ADAPTIVE CONTROL

Besides $\boldsymbol{e}_y$, the passivity-based adaptive control law also uses $\boldsymbol{u}_m$ and $\boldsymbol{x}_m$ in a feedforward configuration, to calculate the control input force accordingly to the simple adaptive control methodology [11]

$$\boldsymbol{u} = \boldsymbol{K}_e(t)\boldsymbol{e}_y + \boldsymbol{K}_x(t)\boldsymbol{x}_m + \boldsymbol{K}_u(t)\boldsymbol{u}_m \tag{32}$$

where $\boldsymbol{K}_e(t) \in \mathbb{R}^{3\times3}$ represents the adaptive control gain that maintains stability of the closed-loop system, and $\boldsymbol{K}_x(t) \in \mathbb{R}^{3\times6}$ and $\boldsymbol{K}_u(t) \in \mathbb{R}^{3\times3}$ are adaptive feedforward control gains contributing to bringing $\boldsymbol{e}_y$ asymptotically to zero without requiring excessively large values of $\boldsymbol{K}_e(t)$.

A. Decentralized Direct Adaptation Law

The direct adaptation law is based on the decentralized simple adaptive control (DSAC) methodology [8], [9], which calculates the integral terms of these gains to achieve a steepest descent minimization of the tracking errors

$$\dot{\boldsymbol{K}}_{Ix}(t) = \boldsymbol{R}^T\text{diag}\left\{\boldsymbol{R}\boldsymbol{e}_y\boldsymbol{x}_m^T\right\}\Gamma_{Ix} \tag{33}$$

$$\dot{\boldsymbol{K}}_{Iu}(t) = \text{diag}\left\{\boldsymbol{e}_y\boldsymbol{u}_m^T\right\}\Gamma_{Iu} \tag{34}$$

with

$$\boldsymbol{R}=\begin{bmatrix}\boldsymbol{I}_3\\ \boldsymbol{I}_3\end{bmatrix}\in\mathbb{R}^{6\times 3} \tag{35}$$

where $\Gamma_{Iu}\in\mathbb{R}^{3\times 3}$ and $\Gamma_{Ix}\in\mathbb{R}^{6\times 6}$ denote the positive-definite diagonal matrices that set the adaptation rate of the feedforward adaptive gains, that is, the rate at which the gains are allowed to vary, and where diag $\{\boldsymbol{W}\}$ denotes the diagonalization operation on a square matrix $\boldsymbol{W}\in\mathbb{R}^{n\times n}$ whose elements are denoted $w_{i,j}$, as follows

$$\text{diag}\{\boldsymbol{W}\}=\begin{bmatrix}w_{1,1} & 0 & \cdots & 0\\ 0 & w_{2,2} & \cdots & 0\\ \vdots & \vdots & \ddots & \vdots\\ 0 & 0 & \cdots & w_{n,n}\end{bmatrix} \tag{36}$$

The integral term of $\boldsymbol{K}_e(t)$ is calculated in a similar way

$$\dot{\boldsymbol{K}}_{Ie}(t)=\text{diag}\left\{\boldsymbol{e}_y\boldsymbol{e}_y^T\right\}\Gamma_{Ie} \tag{37}$$

where $\Gamma_{Ie}\in\mathbb{R}^{3\times 3}$ sets the adaptation rate of $\boldsymbol{K}_{Ie}(t)$. While only the integral terms above are necessary to guarantee the closed-loop stability, proportional terms are also considered since they are known to increase the rate of asymptotic convergence. These proportional terms are calculated given by

$$\begin{aligned}\boldsymbol{K}_{Pe}(t) &= \text{diag}\left\{\boldsymbol{e}_y\boldsymbol{e}_y^T\right\}\Gamma_{Pe} && (38)\\ \boldsymbol{K}_{Px}(t) &= \boldsymbol{R}^T\text{diag}\left\{\boldsymbol{R}\boldsymbol{e}_y\boldsymbol{x}_m^T\right\}\Gamma_{Px} && (39)\\ \boldsymbol{K}_{Pu}(t) &= \text{diag}\left\{\boldsymbol{e}_y\boldsymbol{u}_m^T\right\}\Gamma_{Pu} && (40)\end{aligned}$$

where $\Gamma_{Pe},\Gamma_{Pu}\in\mathbb{R}^{3\times 3}$ and $\Gamma_{Px}\in\mathbb{R}^{6\times 6}$ are the constant coefficient matrices. Finally, the three adaptive gains in the control law given by Eq. (32) are obtained by adding the integral terms to the proportional terms

$$\begin{aligned}\boldsymbol{K}_e(t) &= \boldsymbol{K}_{Pe}(t)+\boldsymbol{K}_{Ie}(t) && (41)\\ \boldsymbol{K}_x(t) &= \boldsymbol{K}_{Px}(t)+\boldsymbol{K}_{Ix}(t) && (42)\\ \boldsymbol{K}_u(t) &= \boldsymbol{K}_{Pu}(t)+\boldsymbol{K}_{Iu}(t) && (43)\end{aligned}$$

The adaptive law can be rewritten concisely as

$$\boldsymbol{u}=\boldsymbol{K}(t)\boldsymbol{r} \tag{44}$$

where $\boldsymbol{K}(t)\in\mathbb{R}^{3\times 12}$ and $\boldsymbol{r}\in\mathbb{R}^{12\times 1}$ are given by

$$\begin{aligned}\boldsymbol{K}(t) &= \boldsymbol{K}_P(t)+\boldsymbol{K}_I(t) && (45)\\ \boldsymbol{r} &= \begin{bmatrix}\boldsymbol{e}_y^T & \boldsymbol{x}_m^T & \boldsymbol{u}_m^T\end{bmatrix}^T && (46)\end{aligned}$$

With this representation, $\boldsymbol{K}_P(t),\boldsymbol{K}_I(t)\in\mathbb{R}^{3\times 12}$ are simply

$$\boldsymbol{K}_P(t)=\boldsymbol{S}^T\text{diag}\left\{\boldsymbol{S}\boldsymbol{e}_y\boldsymbol{r}^T\right\}\Gamma_P \tag{47}$$

$$\dot{\boldsymbol{K}}_I(t)=\boldsymbol{S}^T\text{diag}\left\{\boldsymbol{S}\boldsymbol{e}_y\boldsymbol{r}^T\right\}\Gamma_I \tag{48}$$

where $\Gamma_P,\Gamma_I\in\mathbb{R}^{12\times 12}$ are

$$\Gamma_P=\begin{bmatrix}\Gamma_{Pe} & & \\ & \Gamma_{Px} & \\ & & \Gamma_{Pu}\end{bmatrix},\Gamma_I=\begin{bmatrix}\Gamma_{Ie} & & \\ & \Gamma_{Ix} & \\ & & \Gamma_{Iu}\end{bmatrix}$$

and the matrix $\boldsymbol{S}\in\mathbb{R}^{12\times 3}$ is

$$\boldsymbol{S}=\begin{bmatrix}\boldsymbol{I}_3 & \boldsymbol{I}_3 & \boldsymbol{I}_3 & \boldsymbol{I}_3\end{bmatrix}^T \tag{49}$$

B. Ideal States, Control Input and Feedforward Gains

Perfect tracking, i.e., $\boldsymbol{y}$ tracks $\boldsymbol{y}_m$, is obtained when the plant is said to be the *ideal* plant, which implies that it moves along the bounded ideal states, denoted by $\boldsymbol{x}^*\in\mathbb{R}^6$. In other words, the ideal plant dynamics

$$\dot{\boldsymbol{x}}^*=\boldsymbol{A}^*\boldsymbol{x}^*+\boldsymbol{B}\boldsymbol{u}^*+\boldsymbol{G}^*,\qquad \boldsymbol{y}_m=\boldsymbol{C}\boldsymbol{x}^* \tag{50}$$

moves along $\boldsymbol{x}^*$, where $\boldsymbol{A}^*\equiv\boldsymbol{A}(\boldsymbol{x}^*)$ and $\boldsymbol{G}^*\equiv\boldsymbol{G}(\boldsymbol{x}^*)$. Note that $\boldsymbol{x}^*$ must be distinguished from $\boldsymbol{x}_m$ since the order of $\boldsymbol{x}^*$ always matches that of $\boldsymbol{x}$, which may be (possibly) very large, whereas $\boldsymbol{x}_m$ can be of any order, just sufficiently large to generate the desired output signal $\boldsymbol{y}_m$. In Eq. (50), $\boldsymbol{u}^*\in\mathbb{R}^3$ denotes the ideal control input obtained when perfect tracking occurs, that is, whenever the tracking error $\boldsymbol{e}_y$ is zero. In other words, this ideal control input thus keeps the plant along $\boldsymbol{x}^*$ which allows perfect tracking. In view of the above, $\boldsymbol{u}^*$ is given by

$$\boldsymbol{u}^*=\tilde{\boldsymbol{K}}_x\boldsymbol{x}_m+\tilde{\boldsymbol{K}}_u\boldsymbol{u}_m \tag{51}$$

where $\tilde{\boldsymbol{K}}_x\in\mathbb{R}^{3\times 6}$ and $\tilde{\boldsymbol{K}}_u\in\mathbb{R}^{3\times 3}$ are the constant ideal feedforward control gains, which are fictitious, not needed for implementation. As such, they represent the constant gain values that result in perfect tracking, that is

$$\boldsymbol{e}_y=\boldsymbol{0}_3 \tag{52}$$

Otherwise, there is a non-zero state error $\boldsymbol{e}_x(t)\in\mathbb{R}^6$, which is defined as

$$\boldsymbol{e}_x\triangleq\boldsymbol{x}^*-\boldsymbol{x} \tag{53}$$

In turn, $\boldsymbol{e}_y$ is no longer equal to zero, and is obtained as

$$\boldsymbol{e}_y=\boldsymbol{C}\boldsymbol{x}^*-\boldsymbol{C}\boldsymbol{x}=\boldsymbol{C}\boldsymbol{e}_x \tag{54}$$

The time derivative of Eq. (53) is

$$\begin{aligned}\dot{\boldsymbol{e}}_x &= \left(\boldsymbol{A}-\boldsymbol{B}\tilde{\boldsymbol{K}}_e\boldsymbol{C}\right)\boldsymbol{e}_x+(\boldsymbol{A}^*-\boldsymbol{A})\boldsymbol{x}^*+(\boldsymbol{G}^*-\boldsymbol{G})\\ &\quad -\boldsymbol{B}\,\boldsymbol{K}_P(t)\boldsymbol{r}-\boldsymbol{B}\left(\boldsymbol{K}_I(t)-\tilde{\boldsymbol{K}}\right)\boldsymbol{r} && (55)\end{aligned}$$

where $\tilde{\boldsymbol{K}}\in\mathbb{R}^{3\times 12}$ is defined as

$$\tilde{\boldsymbol{K}}\triangleq\begin{bmatrix}\tilde{\boldsymbol{K}}_e & \tilde{\boldsymbol{K}}_x & \tilde{\boldsymbol{K}}_u\end{bmatrix} \tag{56}$$

C. Stability

Theorem 2. The passivity-based adaptive controller in Eq. (32) with the decentralized adaptation laws given in Eqs. (33)-(43), applied to the square nonlinear spacecraft relative dynamics representation Eq. (7) satisfying the ASP conditions, guarantees the boundeness of all adaptive gains and asymptotic convergence of the state and output tracking errors, in the sense that

$$\|\boldsymbol{e}_y\| \to 0 \quad \text{and} \quad \|\boldsymbol{e}_x\| \to 0 \quad \text{as} \quad t \to \infty$$

where $\|\cdot\|$ corresponds to the standard L^2 norm.

Proof. Let define V as a continuously differentiable positive-definite symmetric function

$$V = \boldsymbol{e}_x^T \boldsymbol{P}\, \boldsymbol{e}_x + \mathrm{tr}\left[\left(\boldsymbol{K}_I(t) - \tilde{\boldsymbol{K}}\right)\Gamma_I^{-1}\left(\boldsymbol{K}_I(t) - \tilde{\boldsymbol{K}}\right)^T\right] \tag{57}$$

Making use of the ASP conditions (23) and (24), the time-derivative of Eq. (57) is

$$\begin{aligned}\dot{V} \;=\; & -\boldsymbol{e}_x^T \boldsymbol{Q} \boldsymbol{e}_x \\ & - 2\mathbf{e}_x^T \boldsymbol{C}^T \boldsymbol{S}^T \mathrm{diag}\left\{\boldsymbol{S}\boldsymbol{C}\boldsymbol{e}_x \boldsymbol{r}^T\right\}\Gamma_P \boldsymbol{r} \\ & + 2\boldsymbol{e}_x^T \boldsymbol{P}\left[(\boldsymbol{A}^* - \boldsymbol{A})\,\boldsymbol{x}^* + (\boldsymbol{G}^* - \boldsymbol{G})\right]\end{aligned} \tag{58}$$

The positive term needs to be canceled, that is

$$\boldsymbol{e}_x^T \boldsymbol{P}\left[(\boldsymbol{A}^* - \boldsymbol{A})\,\boldsymbol{x}^* + (\boldsymbol{G}^* - \boldsymbol{G})\right] = 0 \tag{59}$$

A close look at this condition reveals that any given state $\left\{\begin{array}{cccccc} x & y & z & \dot{x} & \dot{y} & \dot{z}\end{array}\right\}$, requires the existence of solutions for one equation with six unknowns $\left\{\begin{array}{cccccc} x^* & y^* & z^* & \dot{x}^* & \dot{y}^* & \dot{z}^*\end{array}\right\}$. In general, this condition implies that for any n-order $\boldsymbol{x}$, there exists an n-order $\boldsymbol{x}^*$, such that this equation is satisfied. In general, this condition is satisfied [14], which allows Eq. (58) to be simplified to

$$\begin{aligned}\dot{V} \;=\; & -\boldsymbol{e}_x^T \boldsymbol{Q} \boldsymbol{e}_x \\ & - 2\mathbf{e}_x^T \boldsymbol{C}^T \boldsymbol{S}^T \mathrm{diag}\left\{\boldsymbol{S}\boldsymbol{C}\boldsymbol{e}_x \boldsymbol{r}^T\right\}\Gamma_P \boldsymbol{r}\end{aligned} \tag{60}$$

The Lyapunov derivative in Eq. (60) only includes the state error $\boldsymbol{e}_x$ and is therefore negative definite in $\boldsymbol{e}_x$ and negative semi-definite in the state-gain space $[\boldsymbol{e}_x, \boldsymbol{K}_I(t)]$. Thus, the stability of the adaptive system with respect to boundedness is guaranteed by the Lyapunov direct method [12], and all state and output errors, and adaptive control gains are bounded.

Furthermore, asymptotic stability of the tracking errors is demonstrated by invoking LaSalle's invariance principle for non-autonomous systems [11], [13], which states that for a negative semi-definite Lyapunov derivative of the form of Eq. (60), all system trajectories are contained within the domain $\Omega_0 = \{[\boldsymbol{e}_x, \boldsymbol{K}_I(t)] | \, V([\boldsymbol{e}_x, \boldsymbol{K}_I(t)], t) \leq V([\boldsymbol{e}_{x_0}, \boldsymbol{K}_{I_0}(t)], 0)\}$ (where the subscript $\{\}_0$ denotes the initial conditions), and the entire state space $[\boldsymbol{e}_x, \boldsymbol{K}_I(t)]$ ultimately reaches the domain $\Omega_f = \Omega_0 \cap \Omega$, where Ω denotes the domain defined by the Lyapunov derivative identical to zero. In other words, the state space $[\boldsymbol{e}_x, \boldsymbol{K}_I(t)]$ ultimately reaches the domain defined by $\dot{V}([\boldsymbol{e}_x, \boldsymbol{K}_I(t)], t) \equiv 0$ [14]. Because $\dot{V}([\boldsymbol{e}_x, \boldsymbol{K}_I(t)], t)$ is negative definite in $\boldsymbol{e}_x$, the system ends with $\boldsymbol{e}_x \equiv \mathbf{0}$. Finally, since $\boldsymbol{e}_x \equiv \mathbf{0}$ implies $\boldsymbol{e}_x = \boldsymbol{e}_y = \mathbf{0}$, asymptotic stability of the state and output tracking errors is guaranteed.

□

V. SIMULATION RESULTS

The effectiveness and robustness of the proposed formation flying control law was studied in numerical simulations using the nonlinear relative equations of motion given by Eqs. (2)-(6) along with the proposed controller provided in Eq. (32) and associated decentralized adaptation laws in Eqs. (33)-(43). The desired relative motion corresponds to the PCO represented by Eq. (30). The dynamics and orbital parameters used in simulations are given by m_c = 100 kg, $\mu = 398,600$ km^3/s^2, and $a = 7,200$ km. The initial conditions for the relative states are $x_0 = \left[\begin{array}{cccccc} -0.02 \text{ km} & 0 & 0 & 0 & 2e-5 \text{ km/s} & 0\end{array}\right]$. These initial conditions, if the chaser spacecraft was left uncontrolled, would would not naturally lead to the desired PCO relative motion, but would rather lead to a passive in-plane elliptical formation. The control parameters were selected as

$$\begin{aligned}\Gamma_{Pe} &= \Gamma_{Ie} = 10e5\boldsymbol{I}_3 \\ \Gamma_{Px} &= 5e3\boldsymbol{I}_6, \quad \Gamma_{Pu} = 5e3\boldsymbol{I}_3 \\ \Gamma_{Ix} &= 10\boldsymbol{I}_6, \quad \Gamma_{Iu} = 10\boldsymbol{I}_3\end{aligned}$$

These parameters were selected to achieve a satisfactory response under nominal design conditions, defined without external disturbances, and a chaser spacecraft m_c = 100 kg. The ideal model was designed with $\zeta = 0.9$ and $\omega_n = 0.13$ rad/s, and the ratio of position to velocity output was selected as $\alpha = 1$. The results obtained with the adaptive controller are compared to a benchmark non-adaptive proportional-derivative controller given by

$$\boldsymbol{u} = \boldsymbol{K}_P \begin{bmatrix} x_d - x \\ y_d - y \\ z_d - z \end{bmatrix} + \boldsymbol{K}_D \begin{bmatrix} \dot{x}_d - \dot{x} \\ \dot{y}_d - \dot{y} \\ \dot{z}_d - \dot{z} \end{bmatrix} \tag{61}$$

where $\boldsymbol{K}_P, \boldsymbol{K}_D \in \mathbb{R}^{3\times3}$ are the control gains tuned to provide good performance under the nominal design conditions defined above. Robustness to off-nominal conditions is verified by applying the same controllers designed under nominal conditions, but to a chaser spacecraft with an uncertain mass and under the influence of unknown disturbances. These off-nominal conditions are defined with $m_c = 200$ kg and with external disturbances defined in [6]. Simulation results under nominal and off-nominal conditions are reported in Fig. 1. As expected, both control approaches yield satisfactory relative motion tracking performance under nominal conditions. However, under off-nominal conditions, the PD controller yields larger trajectory overshoots and sustained oscillations that fail to converge to the desired relative motion, while

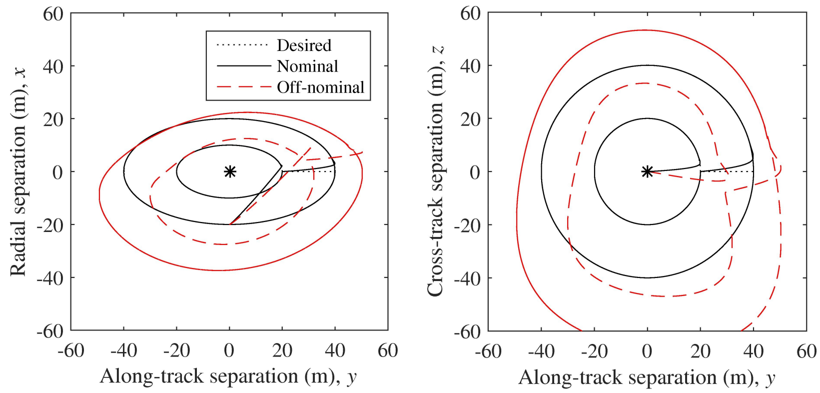

(a) PD controller.

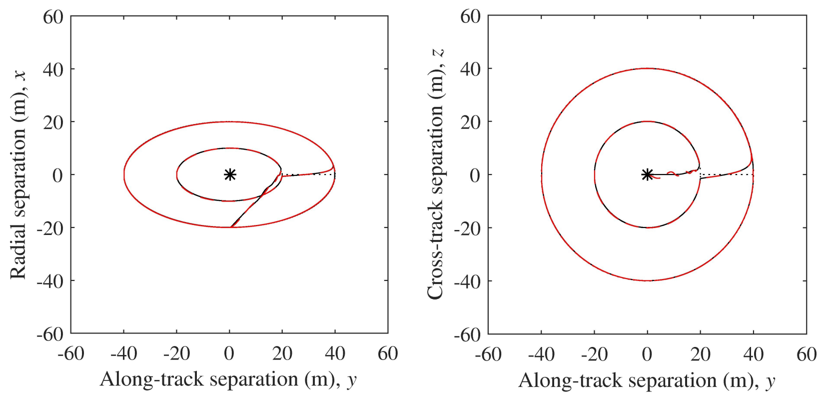

(b) Adaptive controller.

Fig. 1: Relative motion tracking results.

the adaptive controller provides similar responses for both nominal and off-nominal cases, regardless of the presence of the considered uncertainties. This demonstrates the improved robustness achieved with the adaptive strategy.

VI. CONCLUSION

This paper addressed the problem of nonlinear adaptive trajectory control of spacecraft formation flying under dynamics uncertainty and unknown external disturbances. A passivity-based output feedback adaptive control law employing a decentralized adaptation mechanism was proposed, which was shown to satisfy the Almost Strictly Passive conditions that were required for stability demonstration purposes, through Lyapunov direct method and LaSalle's invariance principle arguments. In numerical simulations, the adaptive control strategy proved to be more robust under off-nominal conditions compared to a proportional-derivative controller.

REFERENCES

[1] D. T. Stansbery, and J. R. Cloutier, "Nonlinear Control of Satellite Formation Flight," *AIAA Guidance, Navigation, and Control Conference and Exhibit*, Denver, CO, AIAA Paper 2000–4436, 2000.

[2] R. Kristiansen, and P. J. Nicklasson, "Spacecraft Formation Flying: a Review and New Results on State Feedback Control," *Acta Astronautica*, Vol. 65, 2009, pp. 1537–1552.

[3] M. S. de Queiroz, V. Kapila, and Q. Yan, "Adaptive Nonlinear Control of Multiple Spacecraft Formation Flying," *Journal of Guidance, Control, and Dynamics*, Vol. 23, No. 3, 2000, pp. 385–390.

[4] H. Wong, V. Kapila, and A. G. Sparks, "Adaptive Output Feedback Tracking Control of Spacecraft Formation," *International Journal of Robust and Nonlinear Control*, Vol. 12, Nos. 23, 2002, pp. 117–139.

[5] K. Shahid, and K. D. Kumar, "Satellite Formation Flying Using Variable Structure Model Reference Adaptive Control," *Proceedings of the Institution of Mechanical Engineers*, *Part G* (*Journal of Aerospace Engineering*), Vol. 223, 2009, pp. 271–283.

[6] G. Godard, and K. D. Kumar, "Fault Tolerant Reconfigurable Satellite Formations Using Adaptive Variable Structure Techniques," *Journal of Guidance, Control, and Dynamics*, Vol. 33, No. 3, 2010, pp. 969–984.

[7] K. W. Lee, and S. N. Singh, "Variable-Structure Model Reference Adaptive Formation Control of Spacecraft," *Journal of Guidance, Control, and Dynamics*, Vol. 35, No. 1, 2012, pp. 104–115.

[8] S. Ulrich, J. Z. Sasiadek, and I. Barkana, "On a New Class of Direct Adaptive Output Feedback Controllers for Nonlinear Square Systems," *51st IEEE Conference on Decision and Control*, IEEE, Piscataway, NJ, 2012, pp. 4139–4144.

[9] S. Ulrich, and J. Z. Sasiadek, "Decentralized Simple Adaptive Control of Nonlinear Systems," *International Journal of Adaptive Control and Signal Processing*, Vol. 28, No. 7, 2014, pp. 750–763.

[10] I. Barkana, "Output Feedback Stabilizability and Passivity in Nonstationary and Nonlinear Systems," *International Journal of Adaptive Control and Signal Processing*, Vol. 24, No. 7, 2010, pp. 568–591.

[11] H. Kaufman, I. Barkana, and K. Sobel, *Direct Adaptive Control Algorithms: Theory and Applications*, 2nd ed., Communications and Control Engineering Series, New York, NY: Springer, 1997.

[12] J. J. E. Slotine, and W. Li, *Applied Nonlinear Control*, Prentice Hall, Englewood Cliffs, NJ, 1991, pp. 123–126.

[13] J. P. LaSalle, "Stability of Nonautonomous Systems," *Nonlinear Analysis: Theory, Methods & Applications*, Vol. 1, No. 1, 1976, pp. 83–90.

[14] I. Barkana, "The New Theorem of Stability – Direct Extension of Lyapunov Theorem," *Mathematics in Engineering, Science and Aerospace*, Vol. 6, No. 3, 2015, pp. 519–535.